Collective spin-wave excitations in a two-dimensional array of coupled magnetic nanodots

Roman Verba* and Gennadiy Melkov
Faculty of Radiophysics, Taras Shevchenko National University of Kyiv, Kyiv 01601, Ukraine

Vasil Tiberkevich and Andrei Slavin
Department of Physics, Oakland University, Rochester, Michigan 48309, USA

(Received 13 October 2011; revised manuscript received 21 December 2011; published 23 January 2012)

A general theory of collective spin-wave excitations in a two-dimensional array of magnetic nanodots coupled by magnetodipolar interaction is developed. The theory allows one to analytically calculate spectra, damping rates, excitation efficiencies, and other characteristics of spin waves in both periodic and aperiodic ground states of an array. It is demonstrated that *all* the properties of collective spin waves in an array existing in any *spatially periodic* ground state (e.g., ferromagnetic or chessboard antiferromagnetic) are determined by the *same* state-independent array's demagnetization tensor $\hat{\boldsymbol{F}}_{\boldsymbol{k}}$, which is determined by the spin-wave wave vector $\boldsymbol{k}$, the size and shape of the array's elements (nanodots), and the geometry of the array's lattice. The applications of the developed general theory are illustrated on particular examples: (i) spin waves in ferromagnetic and chessboard antiferromagnetic states of a square array, and (ii) localized spin-wave excitations associated with an isolated "defect" in a uniform ferromagnetic ground state of a square array.

DOI: 10.1103/PhysRevB.85.014427 PACS number(s): 75.75.−c, 75.78.−n, 75.30.Ds

I. INTRODUCTION

Recent advances in the fabrication of patterned magnetic media open a possibility to create large arrays of interacting submicrometer-sized magnetic dots. Such dot arrays are promising candidates for applications not only as bit-patterned magnetic storage media,[1] but, also, as magnonic crystals—artificial structures with periodic variation of magnetic properties. During the past decade the concept of artificial magnonic crystals becomes increasingly popular because these periodic structures have interesting and useful new properties that cannot be achieved in conventional magnetic media. In particular, it has been demonstrated experimentally[2–6] that periodic patterning of a ferromagnetic film leads to a strong modification of the spin-wave spectra and may result in the formation of frequency zones where spin-wave propagation is prohibited. The widths and positions of frequency zones where spin-wave propagation is allowed and prohibited can be controlled by changing the geometric and magnetic parameters of artificial magnonic crystals.

It is important to mention, that the properties of collective spin-wave excitations in artificial magnonic crystals formed by arrays of interacting magnetic nanodots can, in principle, be controlled *dynamically* by dynamical modification of the ground state of the magnetic dot array. It should be noted, that in the absence of an external bias magnetic field the ground state of an individual magnetic nanodot is at least doubly degenerate, because the magnetic energy of the dot is an even function of the dot magnetization. Therefore, there are many possible static configurations in an array of dots under the same external conditions. The magnetodipolar interaction between dots removes the degeneracy of different configurations, leading to the instability of most of them. Nonetheless, even in a relatively simple array of dots, having perpendicular anisotropy, there may be several stable static configurations (ground states) separated by energy barriers. Besides two relatively simple ground states, such as ferromagnetic (when all the magnetic moments are parallel to each other) and chessboard antiferromagnetic (when the magnetic moments of the neighboring dots have opposite directions), there can exist periodic ground states with larger spatial periods (for details see, e.g., Ref. 7). Moreover, a periodic ground state can have point defects or an array can be divided into domains, thus forming states that are nonperiodic (see examples in Fig. 1). Also, in the case of a dot array formed by magnetic dots that are in-plane isotropic (in that case the ground state of an isolated dot is infinitely degenerate) the ground state of an array could be much more complicated.[8–10] Recently, it has been demonstrated experimentally that it is possible to control the ground state, and, therefore, the microwave spin-wave properties of an artificial magnonic crystal by gradually changing an external parameter (e.g., the bias magnetic field).[11,12]

The theoretical investigations of collective spin-wave excitations in arrays of interacting magnetic dots are rather complicated due to the long-range nature of magnetodipolar interaction existing between individual dots. Small dot arrays, consisting of not more than ten dots, were investigated using micromagnetic modeling in the cases of dots having rectangular[13,14] and cylindrical[2,15] shapes. The arrays of long magnetic stripes were analyzed using the method of tensorial Green's functions.[3,16] In the framework of this method the problem is reduced to a system of integral equations that were solved numerically. With some modifications, the same method was applied to calculate the spin-wave spectrum of the array of interacting rectangular dots.[5] Alternatively, collective spin-wave excitations of an array of interacting magnetic elements can be treated as a linear combination of eigenmodes of an isolated magnetic dot. Using this approach, the spin-wave spectra in arrays of spherical magnetic elements[17–19] and rectangular[20] magnetic dots in a saturated state, and arrays of cylindrical dots in a vortex state[21] were calculated. The lowest (gyrotropic) collective mode of an array of dots in a vortex ground state was analyzed using the well-known Thiele's equation in Ref. 22. An approximate analytical theory of a

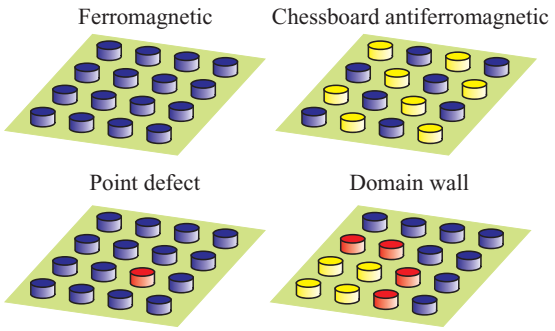

FIG. 1. (Color online) Examples of periodic (upper frames) and aperiodic (lower frames) ground states of an array of magnetic nanodots. Different colors represent different magnetization direction (for the antiferromagnetic state—the directions are opposite).

spin-wave spectrum in infinite periodic arrays of magnetic dots in ferromagnetic and chessboard antiferromagnetic ground states was developed in Refs. 23 and 24 using the Holstein-Primakoff transformation. Within this analytical approach, individual magnetic dots were approximated by pointlike magnetic dipoles. A variant of a similar analytic theory that uses multipole expansion of the dot variable magnetization was developed in Ref. 25.

In our current paper we present a general analytic method that allows one to calculate spin-wave spectra in an arbitrary array of interacting magnetic dots. Although we assume that the magnetization of each individual dot in the array is spatially uniform ("macrospin" approximation), in contrast with the "point-dipole" approximation of Refs. 23 and 24 we take into account real shape-dependent demagnetization fields of individual dots. Of course, the macrospin approximation for the magnetization of individual dots limits the applicability of our dynamic calculations to the case of collective branches of spin-wave spectrum of the array, formed by quasiuniform modes of dots. These branches are expected to be dominant in the microwave response of an array and, therefore, are the most interesting branches from a practical point of view. Our method of calculation of the dipolar interaction between the dots is general and can also be used in the case of spatially nonuniform dot magnetization. In contrast with all the previously used theories, the general analytic approach developed below is applicable to both finite-size and infinite periodic arrays of magnetic dots. In the framework of this analytic approach it is possible to develop a perturbation theory, which allows one to calculate damping rates of the collective spin-wave modes and to build a theory of excitation of these modes by an external microwave magnetic field.

We would like to stress that the analytic understanding of the spectra of collective spin-wave modes in arrays of interacting magnetic dots is not only necessary for the practical applications of magnonic crystals based on these arrays, but also provides information about the stability of the array ground states: usually, when a magnetic order is approaching a critical value for an external parameter (e.g., interdot distance or applied field), one of the collective modes is softening and its frequency vanishes. Therefore, information about the spin-wave spectra is vital for the development of bit-patterned magnetic memory devices.

In the following we restrict our attention to the case of identical magnetic dots, although the developed method is general and can be used in more complicated cases. Also, after formulating the general equations describing the magnetodipolar interactions in a dot array of an arbitrary geometry we consider in more detail the case of a simple array lattice where a unit cell contains only one magnetic dot.

The paper has the following structure. In Sec. II we introduce a mutual demagnetization tensor $\hat{\boldsymbol{N}}(\boldsymbol{r})$ (Refs. 26 and 27) to describe the magnetodipolar interaction between the magnetic nanodots forming the array. In Sec. III we present a general formalism for the description of collective spin-wave excitations in an arbitrary array of magnetic nanodots. The results of this section are general and can be applied, without restrictions, to an arbitrary array of magnetic dots in an arbitrary ground state. Several examples of application of this general formalism are presented in Sec. IV. In particular, we calculate the spectrum of spin waves in a square array of magnetic nanodots (in both ferromagnetic and chessboard antiferromagnetic ground states) and the spectrum of localized spin-wave excitations associated with an isolated "defect" in a periodic ground state of a dot array. Finally, a summary of the obtained results and conclusions are presented in Sec. V.

II. MUTUAL DIPOLAR INTERACTION OF MAGNETIC DOTS

Let us consider magnetodipolar interaction between two magnetic dots separated by the distance $\boldsymbol{r} = \boldsymbol{r}_j - \boldsymbol{r}_k$. The averaged magnetodipolar field created by the dot located at the position $\boldsymbol{r}_k$ (position vector of the dot center) and acting on the dot at the position $\boldsymbol{r}_j$ can be written as[26,27]

$$\boldsymbol{B}_{jk} = -\mu_0 \hat{\boldsymbol{N}}(\boldsymbol{r}_j - \boldsymbol{r}_k) \cdot \boldsymbol{M}_k, \tag{2.1}$$

where μ_0 is the vacuum permeability, $\boldsymbol{M}_k$ is the magnetization vector of the kth dot, and $\hat{\boldsymbol{N}}(\boldsymbol{r})$ is the mutual demagnetization tensor which depends on the size and shape of the dots and the interdot separation $\boldsymbol{r} = \boldsymbol{r}_j - \boldsymbol{r}_k$. In the case $\boldsymbol{r} = \boldsymbol{0}$ the tensor $\hat{\boldsymbol{N}}(\boldsymbol{0})$ coincides with the usual self-demagnetization tensor of the dot.

In a general case, tensor $\hat{\boldsymbol{N}}(\boldsymbol{r})$ can be expressed as the following inverse Fourier transform:[26]

$$N_{\alpha\beta}(\boldsymbol{r}_j - \boldsymbol{r}_k) = \frac{1}{V_j} \int D_j(\boldsymbol{\kappa}) D_k^*(\boldsymbol{\kappa}) \frac{\kappa_\alpha \kappa_\beta}{\kappa^2} e^{i\boldsymbol{\kappa}\cdot(\boldsymbol{r}_j - \boldsymbol{r}_k)} \frac{d^3\boldsymbol{\kappa}}{(2\pi)^3}, \tag{2.2}$$

where $\alpha, \beta \in \{x, y, z\}$ are the Cartesian vector components, V_j is the volume of the jth dot, integration is carried out over the whole three-dimensional $\boldsymbol{\kappa}$ space, and the so-called "shape amplitude"[26] of the dot is defined as

$$D_j(\boldsymbol{\kappa}) = \int_{V_j} e^{-i\boldsymbol{\kappa}\cdot\boldsymbol{r}}\, d^3\boldsymbol{r}. \tag{2.3}$$

In our current paper we are interested in a specific case when the interacting dots are identical and lie in the same x-y plane. Under this restriction, the z component of the separation vector $\boldsymbol{r} = \boldsymbol{r}_j - \boldsymbol{r}_k$ is identically zero. In such a case it is convenient to represent the wave-vector $\boldsymbol{\kappa}$ as a sum of the in-plane wave vector $\boldsymbol{k} = k_x \boldsymbol{e}_x + k_y \boldsymbol{e}_y$ (where $\boldsymbol{e}_\alpha$ is the unit vector in the

α direction) and a perpendicular (to the dot plane) wave vector κ_z: $\boldsymbol{\kappa} = \boldsymbol{k} + \kappa_z \boldsymbol{e}_z$. Performing integration over the perpendicular wave vector κ_z, one can represent the mutual demagnetization tensor $\hat{\boldsymbol{N}}(\boldsymbol{r})$ as a *two-dimensional* Fourier transformation,

$$\hat{\boldsymbol{N}}(\boldsymbol{r}) = \int \hat{\boldsymbol{N}}_{\boldsymbol{k}} e^{i\boldsymbol{k}\cdot\boldsymbol{r}} \frac{d^2\boldsymbol{k}}{(2\pi)^2}, \tag{2.4}$$

where $\hat{\boldsymbol{N}}_{\boldsymbol{k}}$ is the two-dimensional Fourier image of the demagnetization tensor $\hat{\boldsymbol{N}}(\boldsymbol{r})$. Integration over the κ_z can be performed analytically in the case of "planar" dots having constant height h along the z axis, and the tensor $\hat{\boldsymbol{N}}_{\boldsymbol{k}}$ takes the form

$$\hat{\boldsymbol{N}}_{\boldsymbol{k}} = \frac{|\sigma_{\boldsymbol{k}}|^2}{S} \begin{pmatrix} \frac{k_x^2}{k^2} f(kh) & \frac{k_x k_y}{k^2} f(kh) & 0 \\ \frac{k_x k_y}{k^2} f(kh) & \frac{k_y^2}{k^2} f(kh) & 0 \\ 0 & 0 & 1 - f(kh) \end{pmatrix}. \tag{2.5}$$

Here

$$f(kh) = 1 - \frac{1 - \exp(-kh)}{kh}, \tag{2.6}$$

S is the area of the dot, and $\sigma_{\boldsymbol{k}}$ is the Fourier image of the dot's shape in the x-y plane,

$$\sigma_{\boldsymbol{k}} = \int_S e^{-i\boldsymbol{k}\cdot\boldsymbol{r}}\, d^2\boldsymbol{r}, \tag{2.7}$$

where integration goes over the area S of the dot.

In particular, for a circular dot of the radius R we get

$$S = \pi R^2, \quad \sigma_{\boldsymbol{k}} = S \frac{2J_1(kR)}{kR}, \tag{2.8a}$$

where $J_1(x)$ is the Bessel function of the first order. For an elliptical dot having semiaxes a and b (along the x and y axes, respectively) we get

$$S = \pi ab, \quad \sigma_{\boldsymbol{k}} = S \frac{2J_1\left(\sqrt{k_x^2 a^2 + k_y^2 b^2}\right)}{\sqrt{k_x^2 a^2 + k_y^2 b^2}}, \tag{2.8b}$$

and for a rectangular dot having sizes l_x and l_y we obtain

$$S = l_x l_y, \quad \sigma_{\boldsymbol{k}} = S \frac{\sin(k_x l_x/2)}{k_x l_x/2} \frac{\sin(k_y l_y/2)}{k_y l_y/2}. \tag{2.8c}$$

As will be shown below, the Fourier image of the mutual demagnetization tensor $\hat{\boldsymbol{N}}_{\boldsymbol{k}}$ can be directly used for the computationally efficient evaluation of the spin-wave spectra in spatially periodic arrays of magnetic dots.

It is evident from the definitions of the tensors $\hat{\boldsymbol{N}}(\boldsymbol{r})$ and $\hat{\boldsymbol{N}}_{\boldsymbol{k}}$ that they are both real valued and symmetrical with respect to transposition of vector indices and spatial inversion. Namely,

$$\hat{\boldsymbol{N}}(\boldsymbol{r}) = \hat{\boldsymbol{N}}^*(\boldsymbol{r}) = \hat{\boldsymbol{N}}^{\mathrm{T}}(\boldsymbol{r}) = \hat{\boldsymbol{N}}(-\boldsymbol{r}) \tag{2.9a}$$

and

$$\hat{\boldsymbol{N}}_{\boldsymbol{k}} = \hat{\boldsymbol{N}}_{\boldsymbol{k}}^* = \hat{\boldsymbol{N}}_{\boldsymbol{k}}^{\mathrm{T}} = \hat{\boldsymbol{N}}_{-\boldsymbol{k}}. \tag{2.9b}$$

These symmetry relations are important for some of the properties of collective spin excitations in an array of interacting nanodots coupled by magnetodipolar interaction. In addition, one can show that $\mathrm{Tr}[\hat{\boldsymbol{N}}(\boldsymbol{0})] = 1$ and $\mathrm{Tr}[\hat{\boldsymbol{N}}(\boldsymbol{r})] = 0$ for nonoverlapping dots.[27]

Finally, we note that, using the demagnetization tensor $\hat{\boldsymbol{N}}(\boldsymbol{r})$, the dipolar energy of the array can be written in the following compact form:

$$W_{\mathrm{dip}} = \frac{\mu_0 V}{2} \sum_{j,k} \boldsymbol{M}_j \cdot \hat{\boldsymbol{N}}(\boldsymbol{r}_j - \boldsymbol{r}_k) \cdot \boldsymbol{M}_k. \tag{2.10}$$

Note, that a similar approach can also be used to study dipolar interaction between dots having nonuniform profiles of either static and/or dynamic magnetization. In such a case, instead of a single demagnetization tensor, Eq. (2.5), it is necessary to find separate static-static, dynamic-dynamic, and static-dynamic demagnetization tensors, where the Fourier image $\sigma_{\boldsymbol{k}}$ of the dot's shape in Eq. (2.5) is replaced by the Fourier images of the nonuniform spatial profiles of either a static dot magnetization or a particular nonuniform spin-wave mode (static or dynamic cell functions).

III. GENERAL THEORY OF COLLECTIVE SPIN-WAVE EXCITATIONS

A. Principal equations

We consider below a two-dimensional array of identical magnetic dots lying in the x-y plane (see Fig. 2). The dots are arranged in a spatially periodic lattice with basis vectors $\boldsymbol{a}_1$ and $\boldsymbol{a}_2$. The location of a dot in the array is determined by the two-dimensional integer index $j = (j_1, j_2)$, and the two-dimensional position vector of the jth dot (more precisely, the position vector of the center of the jth dot) is given by

$$\boldsymbol{r}_j = j_1 \boldsymbol{a}_1 + j_2 \boldsymbol{a}_2. \tag{3.1}$$

The area of the unit cell of the lattice is equal to

$$S_0 = \boldsymbol{e}_z \cdot (\boldsymbol{a}_1 \times \boldsymbol{a}_2). \tag{3.2}$$

We assume that the basis vectors $\boldsymbol{a}_i$ are ordered in such a way that the area of the unit cell S_0 defined by Eq. (3.2) is positive.

We also assume that the sizes of the interacting magnetic dots are sufficiently small, so that the magnetic state within each dot can be considered to be spatially uniform (i.e., we can use a macrospin approximation for the magnetization in all individual dots). In this case the state of each dot is completely described by one magnetization vector $\boldsymbol{M}_j \equiv \boldsymbol{M}_j(t)$ of a constant magnitude ($|\boldsymbol{M}_j| = M_s$), where M_s is the saturation magnetization.

We would like to note that the macrospin approximation for the dynamic magnetization of the dot is not an essential

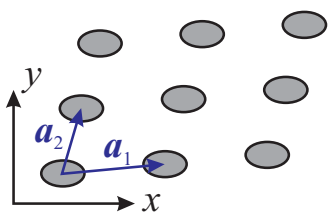

FIG. 2. (Color online) Sketch of the considered array of interacting magnetic dots. The dots lie in the common x-y plane and form a periodic lattice with the basis vectors $\boldsymbol{a}_1$ and $\boldsymbol{a}_2$.

feature of our theoretical approach and can be relaxed if one uses the actual profile of a spin-wave mode existing in each individual magnetic dot when the calculation of the dot's shape amplitude, Eq. (2.3), is performed. This correction will modify the form of the demagnetization tensor $\hat{N}(\boldsymbol{r})$, but will not affect any other calculation results.

Below we consider the case when the dot array is placed in the uniform external bias magnetic field $\boldsymbol{B}_e$ and individual dots are mutually coupled only by the magnetodipolar interaction. For simplicity, we will not consider crystallographic anisotropy—it can be taken into account simply by the renormalization of the self-demagnetization tensor $\hat{N}(\boldsymbol{0})$. The influence of damping and other weak perturbations will be considered in Sec. III C in the framework of the general perturbation theory.

Under the above-formulated approximations, the dynamics of the dots' magnetization vectors $\boldsymbol{M}_j$ is described by the Landau-Lifshits equation

$$\frac{d\boldsymbol{M}_j}{dt} = \gamma(\boldsymbol{B}_{\text{eff},j} \times \boldsymbol{M}_j), \tag{3.3}$$

where $\gamma \approx 2\pi \cdot 28$ GHz/T is the modulus of the gyromagnetic ratio for electron spin, and the effective magnetic field $\boldsymbol{B}_{\text{eff},j}$ consisting of the external bias field and magnetodipolar field created by other dots is given by

$$\boldsymbol{B}_{\text{eff},j} = \boldsymbol{B}_e - \mu_0 \sum_k \hat{N}(\boldsymbol{r}_j - \boldsymbol{r}_k) \cdot \boldsymbol{M}_k. \tag{3.4}$$

The total magnetic energy of the array under our assumptions has the form

$$W = -V \sum_j \boldsymbol{B}_e \cdot \boldsymbol{M}_j + \frac{\mu_0 V}{2} \sum_{j,k} \boldsymbol{M}_j \cdot \hat{N}(\boldsymbol{r}_j - \boldsymbol{r}_k) \cdot \boldsymbol{M}_k. \tag{3.5}$$

B. General formalism for collective spin-wave excitations in the dot array

Magnetization of the jth dot in a stationary ground state can be written as $\boldsymbol{M}_j = M_s \boldsymbol{\mu}_j$, where $\boldsymbol{\mu}_j$ is a unit vector in the direction of the dot static magnetization. Vectors $\boldsymbol{\mu}_j$ are determined from the system of equations

$$B_j \boldsymbol{\mu}_j = \boldsymbol{B}_e - \mu_0 M_s \sum_k \hat{N}(\boldsymbol{r}_j - \boldsymbol{r}_k) \cdot \boldsymbol{\mu}_k, \tag{3.6}$$

where B_j is the intrinsic scalar magnetic field acting on the jth dot.

To find the dynamical equations describing small (linear) magnetization excitations of the dot array, we shall use the following ansatz for the dot magnetization:

$$\boldsymbol{M}_j = M_s(\boldsymbol{\mu}_j + \boldsymbol{m}_j) + O(|\boldsymbol{m}_j|^2), \tag{3.7}$$

where $\boldsymbol{m}_j$ is the small dimensionless deviation of the magnetization of the jth dot from the static equilibrium (ground) state described by the vector $\boldsymbol{\mu}_j$. The condition of conservation of the length of magnetization vector $\boldsymbol{M}_j$ in each dot requires the orthogonality of vectors $\boldsymbol{\mu}_j$ and $\boldsymbol{m}_j$,

$$\boldsymbol{\mu}_j \cdot \boldsymbol{m}_j = 0. \tag{3.8}$$

Substituting Eq. (3.7) for $\boldsymbol{M}_j$ in Eq. (3.3), using Eqs. (3.6) and (3.8), and keeping only the terms that are linear in $\boldsymbol{m}_j$, one obtains the following dynamical equations for $\boldsymbol{m}_j$:

$$\frac{d\boldsymbol{m}_j}{dt} = \boldsymbol{\mu}_j \times \sum_k \hat{\Omega}_{jk} \cdot \boldsymbol{m}_k. \tag{3.9}$$

Here the tensor operator $\hat{\Omega}_{jk}$ is defined by the equation

$$\hat{\Omega}_{jk} = \gamma B_j \delta_{jk} \hat{I} + \gamma \mu_0 M_s \hat{N}(\boldsymbol{r}_j - \boldsymbol{r}_k), \tag{3.10}$$

where δ_{jk} is the Kronecker delta ($\delta_{jk} = 1$ for $j = k$ and $\delta_{jk} = 0$ otherwise) and $\hat{I}$ is the identity matrix. It is clear that the tensor operator $\hat{\Omega}_{jk}$ is self-adjoint (in the sense $\hat{\Omega}_{jk} = \hat{\Omega}^{\mathrm{T}}_{kj}$), is symmetric with respect to spatial inversion ($\hat{\Omega}_{jk} = \hat{\Omega}_{kj}$), and has the dimension of frequency.

Note, that the changes to the magnetic energy due to the spin-wave excitations $\boldsymbol{m}_j$ can also be expressed through the tensor $\hat{\Omega}_{jk}$:

$$\Delta W = \frac{M_s V}{2\gamma} \sum_{j,k} \boldsymbol{m}_j \cdot \hat{\Omega}_{jk} \cdot \boldsymbol{m}_k. \tag{3.11}$$

The spin-wave frequencies ω_ν and the profiles of collective spin-wave modes $\boldsymbol{m}_{\nu,j}$ can be found as eigenvalues and eigenvectors of Eq. (3.9), respectively:

$$-i\omega_\nu \boldsymbol{m}_{\nu,j} = \boldsymbol{\mu}_j \times \sum_k \hat{\Omega}_{jk} \cdot \boldsymbol{m}_{\nu,k}. \tag{3.12}$$

Here ν is an index or set of indices used to enumerate different spin-wave modes.

The main properties of the collective spin-wave excitations of the array of dots follow from the properties of the eigenvalue problem, Eq. (3.12), and from the fact that the tensor $\hat{\Omega}_{jk}$ is real and self-adjoint. In particular, it can be shown that the eigenvectors $\boldsymbol{m}_{\nu,j}$ satisfy the following relation:

$$(\omega^*_{\nu'} - \omega_\nu) \sum_j \boldsymbol{m}^*_{\nu',j} \cdot \boldsymbol{\mu}_j \times \boldsymbol{m}_{\nu,j} = 0, \tag{3.13}$$

where the superscript * denotes complex conjugation. Then, for $\nu' = \nu$, the eigenvalues are real, $\omega^*_\nu = \omega_\nu$, unless $\sum_j \boldsymbol{m}^*_{\nu,j} \cdot \boldsymbol{\mu}_j \times \boldsymbol{m}_{\nu,j} = 0$. The latter condition can be satisfied only if the stationary configuration $\boldsymbol{\mu}_j$ (ground state) corresponds to a saddle point of the magnetic energy W, Eq. (3.5). Such magnetization states are unstable, so they cannot be realized in practice, and we will not consider them below. Then, Eq. (3.13) means that the frequencies of collective spin-wave eigenmodes are real, and different eigenmodes $\boldsymbol{m}_{\nu,j}$ are orthogonal in the sense

$$\sum_j \boldsymbol{m}^*_{\nu',j} \cdot \boldsymbol{\mu}_j \times \boldsymbol{m}_{\nu,j} = -iA_\nu \delta_{\nu,\nu'}, \tag{3.14}$$

where A_ν are real constants dependent on the normalization of the eigenvectors $\boldsymbol{m}_{\nu,j}$. We would like to stress that the orthogonality condition, Eq. (3.14), holds even for the nonuniform ground states of the array, i.e., when different dots have different equilibrium directions of magnetization $\boldsymbol{\mu}_j$.

Another orthogonality-type relation for spin-wave modes $\boldsymbol{m}_{\nu,j}$ is

$$\sum_{j,k} \boldsymbol{m}^*_{\nu',j} \cdot \hat{\boldsymbol{\Omega}}_{jk} \cdot \boldsymbol{m}_{\nu,k} = \omega_\nu A_\nu \delta_{\nu,\nu'}. \tag{3.15}$$

This property is useful in approximate calculations of the spin-wave frequencies.[28]

Taking complex conjugate of Eq. (3.12) and using the fact that the tensors $\hat{\boldsymbol{\Omega}}_{jk}$ are real it is easy to show that, if $\boldsymbol{m}_{\nu,j}$ is an eigenvector with an eigenfrequency ω_ν, then $\boldsymbol{m}^*_{\nu,j}$ is also an eigenvector with an eigenfrequency $-\omega_\nu$. Such double degeneracy of spin-wave eigenmodes arises from the fact that the magnetization vectors $\boldsymbol{m}_j$ are real quantities, and their spectra contain both positive and negative frequency components. Only half of the formal solutions of Eq. (3.12) describe "physical" modes $\boldsymbol{m}_{\nu,j}$, while the rest of the solutions are the formal "conjugated" modes $\boldsymbol{m}^*_{\nu,j}$ that guarantee that the vectors $\boldsymbol{m}_j$ are real valued.

The physical modes $\boldsymbol{m}_{\nu,j}$ have positive norms $A_\nu > 0$, whereas the "conjugated" ones have negative norms $-A_\nu$. This can be seen from the general eigenmode expansion of the magnetization vectors $\boldsymbol{m}_j(t)$:

$$\boldsymbol{m}_j(t) = \sum_\nu [\boldsymbol{m}_{\nu,j} c_\nu(t) + \text{c.c.}]. \tag{3.16}$$

Here $c_\nu(t)$ is the complex amplitude of the νth mode, the summation goes *only* over the physical spin-wave modes having $A_\nu > 0$, and c.c. denotes complex conjugated terms (which include all conjugated modes). Substituting the expansion, Eq. (3.16), into the expression for energy, Eq. (3.11), and using Eqs. (3.12) and (3.14) one can write ΔW as

$$\Delta W = \frac{M_s V}{\gamma} \sum_\nu \omega_\nu A_\nu |c_\nu|^2. \tag{3.17}$$

If the equilibrium magnetization configuration $\boldsymbol{\mu}_j$ corresponds to a local minimum of magnetic energy, then ΔW is positive-definite, and the physical modes ($A_\nu > 0$) have positive frequencies $\omega_\nu > 0$. On the other hand, if we formally consider dynamics near a *maximum* of magnetic energy, then $\Delta W < 0$ and the frequencies of the spin-wave modes will be negative $\omega_\nu < 0$, which corresponds to the precession of the magnetization vector in the opposite direction. Thus, Eq. (3.17) gives a convenient tool for the investigation of ground-state stability—only the states having all the ω_ν real and $\omega_\nu A_\nu > 0$ are stable.

The general spin-wave formalism presented above can be used for effective numerical calculations of the spin-wave spectra in finite arrays of magnetic dots in an arbitrary ground state. It follows from Eq. (3.12) that the problem of calculation of the spin-wave spectrum of a dot array can be reduced to a standard task of finding eigenvalues and eigenvectors of a Hamiltonian matrix. In the case when the ground state of an array is periodic (e.g., ferromagnetic or antiferromagnetic), the theory can be further simplified and such cases are considered in Secs. III D and III E.

C. Perturbation theory for spin-wave modes

Magnetic damping and other weak perturbative effects neglected in Eq. (3.3) can be effectively considered in the framework of a spin-wave perturbation theory. In a general case, the perturbed equations for dot magnetization vectors $\boldsymbol{M}_j(t)$ can be written as

$$\frac{d\boldsymbol{M}_j}{dt} = \gamma(\boldsymbol{B}_{\text{eff},j} \times \boldsymbol{M}_j) + \gamma(\boldsymbol{b}_j \times \boldsymbol{M}_j), \tag{3.18}$$

where $\boldsymbol{b}_j$ is the effective field of the perturbation which may depend both on time and the dot magnetizations $\boldsymbol{M}_k$. Considering only the linear processes, we can expand the magnetization of each dot in a series of spin-wave eigenmodes:

$$\boldsymbol{M}_j(t) = M_s \left\{ \boldsymbol{\mu}_j + \sum_\nu [\boldsymbol{m}_{\nu,j} c_\nu(t) + \text{c.c.}] \right\}. \tag{3.19}$$

Here and below the summation over the index ν goes only over the physical modes ($A_\nu > 0$). Substituting Eq. (3.19) for $\boldsymbol{M}_j(t)$ in Eq. (3.18) and using the orthogonality properties of spin-wave eigenmodes $\boldsymbol{m}_{\nu,j}$, one can obtain the perturbed equations for the spin-wave amplitudes $c_\nu(t)$:

$$\frac{dc_\nu}{dt} = -i\omega_\nu c_\nu + i\gamma b_\nu - i\gamma \sum_{\nu'} (S_{\nu,\nu'} c_{\nu'} + \tilde{S}_{\nu,\nu'} c^*_{\nu'}), \tag{3.20}$$

with the following coefficients:

$$b_\nu = \frac{1}{A_\nu} \sum_j \boldsymbol{m}^*_{\nu,j} \cdot \boldsymbol{b}_j, \tag{3.21a}$$

$$S_{\nu,\nu'} = \frac{1}{A_\nu} \sum_j (\boldsymbol{m}^*_{\nu,j} \cdot \boldsymbol{m}_{\nu',j})(\boldsymbol{\mu}_j \cdot \boldsymbol{b}_j), \tag{3.21b}$$

$$\tilde{S}_{\nu,\nu'} = \frac{1}{A_\nu} \sum_j (\boldsymbol{m}^*_{\nu,j} \cdot \boldsymbol{m}^*_{\nu',j})(\boldsymbol{\mu}_j \cdot \boldsymbol{b}_j). \tag{3.21c}$$

In the case when the field $\boldsymbol{b}_j$ of perturbation depends on the magnetization vectors, one should retain in Eq. (3.20) only the terms of the zeroth and first order in c_ν.

The general equation (3.20) allows one to analyze the influence of any type of small perturbations on the spin waves in a dot array.

As an example of such perturbative analysis we consider below two practically important cases: weak damping of collective spin-wave modes and their excitation by an external microwave magnetic field. In the former case, the perturbation field that is created by the Gilbert damping has the form $\boldsymbol{b}_j = -(\alpha_G/\gamma M_s) d\boldsymbol{M}_j/dt$, where α_G is the Gilbert damping parameter. Taking into account that $dc_\nu/dt = -i\omega_\nu c_\nu + O(\alpha_G)$, one can derive the following first-order perturbative equation for the spin-wave amplitudes:

$$\frac{dc_\nu}{dt} = -i\omega_\nu c_\nu - \sum_{\nu'} \Gamma_{\nu,\nu'} c_{\nu'}. \tag{3.22}$$

Here

$$\Gamma_{\nu,\nu'} = \alpha_G \omega_{\nu'} \left(\frac{1}{A_\nu} \sum_j \boldsymbol{m}^*_{\nu,j} \cdot \boldsymbol{m}_{\nu',j} \right). \tag{3.23}$$

If there is no frequency degeneracy among the spin-wave modes, Eq. (3.22) is simplified to the usual form of equation describing damped oscillations with the damping rate $\Gamma_\nu = \Gamma_{\nu,\nu}$. In a degenerate case, one should also take into

account the off-diagonal terms $\nu' \neq \nu$ for proper description of the magnetic damping. As one can see from Eq. (3.23), the difference between the damping rate Γ_ν and $\alpha_G \omega_\nu$ is determined by the ellipticity of the excited spin-wave mode.

The direct excitation of spin waves by an external microwave field is described by the perturbation terms $\boldsymbol{b}_j = (\boldsymbol{b}_{e,j} e^{-i\omega t} + \text{c.c.})$. With the account of magnetic damping (assuming a nondegenerate case) the dynamic equations for c_ν can be written as

$$\frac{dc_\nu}{dt} = -i\omega_\nu c_\nu - \Gamma_\nu c_\nu + i\gamma b_{e,\nu} e^{-i\omega t}, \tag{3.24}$$

where

$$b_{e,\nu} = \frac{1}{A_\nu} \sum_j \boldsymbol{m}^*_{\nu,j} \cdot \boldsymbol{b}_{e,j}. \tag{3.25}$$

Then, the stationary amplitude of the νth mode is given by

$$c_\nu = \frac{\gamma b_{e,\nu}}{\omega_\nu - \omega - i\Gamma_\nu}. \tag{3.26}$$

Using the above expressions, one can easily calculate the microwave absorbtion spectra of an array of interacting magnetic dots. In particular, in a practically important case of a spatially uniform external microwave field, $\boldsymbol{b}_{e,j} = \boldsymbol{b}_e$, the microwave power absorbed by the dot array is given by

$$P = \frac{\omega V N_d}{\mu_0} \boldsymbol{b}^*_e \cdot \hat{\boldsymbol{\chi}}''(\omega) \cdot \boldsymbol{b}_e, \tag{3.27}$$

where N_d is the number of dots in the array and the effective array permeability tensor $\hat{\boldsymbol{\chi}}(\omega) = \hat{\boldsymbol{\chi}}'(\omega) + i\hat{\boldsymbol{\chi}}''(\omega)$ is given by

$$\hat{\boldsymbol{\chi}}(\omega) = \gamma\mu_0 M_s \sum_\nu \frac{\hat{\boldsymbol{\chi}}_\nu}{(\omega_\nu - \omega) - i\Gamma_\nu}, \tag{3.28a}$$

$$\hat{\boldsymbol{\chi}}_\nu = \frac{1}{N_d A_\nu} \sum_{j,k} \boldsymbol{m}^*_{\nu,j} \otimes \boldsymbol{m}_{\nu,k}. \tag{3.28b}$$

where $\otimes$ indicates direct Cartesian product of vectors.

Thus, all the practically important characteristics of an array of magnetic dots can be easily found provided one knows the frequencies ω_ν of the collective spin-wave eigenmodes and the corresponding eigenmode profiles $\boldsymbol{m}_{\nu,j}$.

D. Collective spin waves of an array in a ferromagnetic ground state

When the ground state of an infinite array of magnetic dots is ferromagnetic, the equilibrium directions of magnetization of all dots are identical, $\boldsymbol{\mu}_j = \boldsymbol{\mu}$. Therefore, the internal fields in all the dots are the same, $B_j = B$, and are determined by

$$B\boldsymbol{\mu} = \boldsymbol{B}_e - \mu_0 M_s \sum_{\boldsymbol{r} \in \mathcal{L}} \hat{\boldsymbol{N}}(\boldsymbol{r}) \cdot \boldsymbol{\mu}. \tag{3.29}$$

Here $\mathcal{L}$ denotes the lattice of the dot array:

$$\mathcal{L} = \{n_1 \boldsymbol{a}_1 + n_2 \boldsymbol{a}_2 \,|\, n_1 \in \mathbb{Z},\ n_2 \in \mathbb{Z}\}. \tag{3.30}$$

The spin-wave modes in the periodic ferromagnetic ground state of an array have the form of plane waves:

$$\boldsymbol{m}_j = \boldsymbol{m}_{\boldsymbol{k}} e^{i\boldsymbol{k}\cdot\boldsymbol{r}_j}, \tag{3.31}$$

and can be characterized by their wave vectors $\boldsymbol{k}$. The wave vector $\boldsymbol{k}$ lies within the first Brillouin zone of the array's lattice.

Substituting Eq. (3.31) for $\boldsymbol{m}_j$ in Eq. (3.12) we get a simple (and effectively two-dimensional) eigenvalue problem for $\boldsymbol{m}_{\boldsymbol{k}}$ and $\omega_{\boldsymbol{k}}$:

$$-i\omega_{\boldsymbol{k}} \boldsymbol{m}_{\boldsymbol{k}} = \boldsymbol{\mu} \times \hat{\boldsymbol{\Omega}}_{\boldsymbol{k}} \cdot \boldsymbol{m}_{\boldsymbol{k}}, \tag{3.32}$$

where

$$\hat{\boldsymbol{\Omega}}_{\boldsymbol{k}} = \gamma B \hat{\boldsymbol{I}} + \gamma\mu_0 M_s \hat{\boldsymbol{F}}_{\boldsymbol{k}}, \quad \hat{\boldsymbol{F}}_{\boldsymbol{k}} = \sum_{\boldsymbol{r} \in \mathcal{L}} \hat{N}(\boldsymbol{r}) e^{-i\boldsymbol{k}\cdot\boldsymbol{r}}. \tag{3.33}$$

Using a well-known expression that relates the sums over the direct and reciprocal lattices,[29]

$$\sum_{\boldsymbol{r} \in \mathcal{L}} e^{-i\boldsymbol{k}\cdot\boldsymbol{r}} = \frac{(2\pi)^2}{S_0} \sum_{\boldsymbol{K} \in \mathcal{L}^*} \delta(\boldsymbol{k} + \boldsymbol{K}), \tag{3.34}$$

one can rewrite the tensor $\hat{\boldsymbol{F}}_{\boldsymbol{k}}$ in the form

$$\hat{\boldsymbol{F}}_{\boldsymbol{k}} = \frac{1}{S_0} \sum_{\boldsymbol{K} \in \mathcal{L}^*} \hat{\boldsymbol{N}}_{\boldsymbol{k}+\boldsymbol{K}}, \tag{3.35}$$

where $\mathcal{L}^*$ denotes the reciprocal lattice

$$\mathcal{L}^* = \{n_1 \boldsymbol{k}_1 + n_2 \boldsymbol{k}_2 \,|\, n_1 \in \mathbb{Z},\ n_2 \in \mathbb{Z}\}, \tag{3.36}$$

that is formed by the two basis wave vectors

$$\boldsymbol{k}_1 = -\left(\frac{2\pi}{S_0}\right) \boldsymbol{e}_z \times \boldsymbol{a}_2, \quad \boldsymbol{k}_2 = \left(\frac{2\pi}{S_0}\right) \boldsymbol{e}_z \times \boldsymbol{a}_1. \tag{3.37}$$

Here S_0 is the area of the unit cell of the direct lattice $\mathcal{L}$ [see Eq. (3.2)].

The tensor $\hat{\boldsymbol{F}}_{\boldsymbol{k}}$ possesses all the symmetries of the tensor $\hat{\boldsymbol{N}}_{\boldsymbol{k}}$. In addition, it is periodic with the periods of the reciprocal lattice, $\hat{\boldsymbol{F}}_{\boldsymbol{k}} = \hat{\boldsymbol{F}}_{\boldsymbol{k}+\boldsymbol{k}_1} = \hat{\boldsymbol{F}}_{\boldsymbol{k}+\boldsymbol{k}_2}$, and has a unit trace, $\text{Tr}(\hat{\boldsymbol{F}}_{\boldsymbol{k}}) = 1$. In the case of planar magnetic dots, for which the xz and yz components of the tensor $\hat{\boldsymbol{N}}_{\boldsymbol{k}}$ vanish [see Eq. (2.5)], there are only three independent components of the tensor $\hat{\boldsymbol{F}}_{\boldsymbol{k}}$ (e.g., xx, xy, and yy components).

The expression for the tensor $\hat{\boldsymbol{F}}_{\boldsymbol{k}}$, Eq. (3.35), is especially convenient in practical calculations since the Fourier image $\hat{\boldsymbol{N}}_{\boldsymbol{k}}$ of the mutual demagnetization tensor can be found analytically [see Eq. (2.5)] in all the practically important cases. With the help of Eq. (3.35), calculations of the spin-wave spectra of an array of magnetic dots (with account of finite size and real shape of individual dots) are no more difficult than the calculations in models where individual dots are approximated as "point dipoles."[23,24]

Equation (3.32) is identical to the equation for a single macrospin with the effective demagnetization tensor $\hat{\boldsymbol{F}}_{\boldsymbol{k}}$. Choosing a coordinate system $(x'y'z')$, in which the direction of the equilibrium magnetization $\boldsymbol{\mu}$ coincides with the z' axes, the spin-wave frequency $\omega_{\boldsymbol{k}}$ of the collective spin-wave mode in the array can be written as

$$\omega_{\boldsymbol{k}}^2 = \left(\gamma B + \omega_M F_{\boldsymbol{k}}^{(x'x')}\right)\left(\gamma B + \omega_M F_{\boldsymbol{k}}^{(y'y')}\right) - \left(\omega_M F_{\boldsymbol{k}}^{(x'y')}\right)^2, \tag{3.38}$$

where $\omega_M = \gamma\mu_0 M_s$. Note, also, that the equilibrium condition, Eq. (3.29), can be written as

$$B\boldsymbol{\mu} = \boldsymbol{B}_e - \mu_0 M_s \hat{\boldsymbol{F}}_{\boldsymbol{0}} \cdot \boldsymbol{\mu}. \tag{3.39}$$

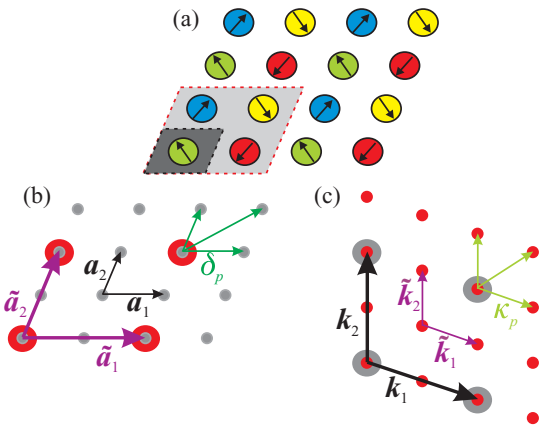

FIG. 3. (Color online) Example of a complex periodic ground state of a magnetic dot array, the so-called noncollinear antiferromagnetic state (Ref. 8). (a) Equilibrium magnetization distribution forming a periodic superlattice $\mathcal{SL}$. The light gray area shows a unit cell of the superlattice $\mathcal{SL}$, which is $P = 4$ times larger than the unit cell of the fundamental lattice $\mathcal{L}$ (dark gray area). (b) Direct lattice $\mathcal{L}$ (small gray circles) formed by the basis vectors $\boldsymbol{a}_1$,$\boldsymbol{a}_2$ and the superlattice $\mathcal{SL}$ (large red circles) formed by the vectors $\tilde{\boldsymbol{a}}_1$,$\tilde{\boldsymbol{a}}_2$. The lattice $\mathcal{L}$ is $P = 4$ times denser than the superlattice $\mathcal{SL}$ and can be restored by translating the superlattice $\mathcal{SL}$ using shift vectors $\boldsymbol{\delta}_p$ (green arrows). (c) Reciprocal lattice $\mathcal{L}^*$ (large gray circles) and reciprocal superlattice $\mathcal{SL}^*$ (small red circles) with basis vectors $\boldsymbol{k}_i$ and $\tilde{\boldsymbol{k}}_i$, respectively. The reciprocal superlattice $\mathcal{SL}^*$ is denser than $\mathcal{L}^*$ and is restored by translating $\mathcal{L}^*$ using shift wave vectors $\boldsymbol{\kappa}_p$ (green arrows).

Thus, the tensor $\hat{\boldsymbol{F}}_{\boldsymbol{k}}$, which we will call the *fundamental tensor* of the array, contains all the necessary information to find both the possible equilibrium ferromagnetic states and the corresponding spectra of the collective spin-wave excitations. As we will show in the following section, the fundamental tensor $\hat{\boldsymbol{F}}_{\boldsymbol{k}}$ contains, also, all the necessary information to find the spin-wave spectra in an arbitrary periodic state of an array of interacting magnetic dots.

E. Collective spin-wave modes of a dot array in a complex periodic ground state

An important class of stationary configurations in an infinite magnetic dot array is formed by periodic nonferromagnetic states [see examples in Figs. 1 and 3(a)]. In such a state the equilibrium magnetizations $\boldsymbol{\mu}_j$ of individual dots form a periodic "superlattice" with basis vectors

$$\tilde{\boldsymbol{a}}_1 = s_{11}\boldsymbol{a}_1 + s_{12}\boldsymbol{a}_2, \quad \tilde{\boldsymbol{a}}_2 = s_{21}\boldsymbol{a}_1 + s_{22}\boldsymbol{a}_2, \tag{3.40}$$

where $s_{ii'}$ are integer numbers. Note, that although the choice of four numbers $s_{ii'}$ completely defines the superlattice, the same superlattice corresponds to many possible choices of $s_{ii'}$. The superlattice is not simple, i.e., its unit cell contains $P > 1$ dots (i.e., the area of the unit cell of the superlattice is PS_0), where

$$P = s_{11}s_{22} - s_{12}s_{21}. \tag{3.41}$$

We assume that P defined by Eq. (3.41) is a positive number, which can always be achieved by proper ordering of the basis vectors $\tilde{\boldsymbol{a}}_i$.

We will denote the superlattice formed by the basis vectors, Eq. (3.40), as $\mathcal{SL}$. Note, that the superlattice $\mathcal{SL}$ is a subset of the fundamental lattice $\mathcal{L}$. In fact, one can define P shift vectors $\boldsymbol{\delta}_p \in \mathcal{L}$, $p \in [1, P]$ in such a way, that the union of the superlattices $\mathcal{SL}$ shifted by $\boldsymbol{\delta}_p$ equals $\mathcal{L}$ [see Fig. 3(b)],

$$\mathcal{L} = \bigcup_p \{\boldsymbol{r} + \boldsymbol{\delta}_p \,|\, \boldsymbol{r} \in \mathcal{SL}\}. \tag{3.42}$$

The reciprocal superlattice, $\mathcal{SL}^*$, is formed using the basis vectors

$$\tilde{\boldsymbol{k}}_1 = -\left(\frac{2\pi}{PS_0}\right)\boldsymbol{e}_z \times \tilde{\boldsymbol{a}}_2 = \left(\frac{s_{22}}{P}\right)\boldsymbol{k}_1 - \left(\frac{s_{21}}{P}\right)\boldsymbol{k}_2, \tag{3.43}$$

$$\tilde{\boldsymbol{k}}_2 = \left(\frac{2\pi}{PS_0}\right)\boldsymbol{e}_z \times \tilde{\boldsymbol{a}}_1 = \left(\frac{s_{11}}{P}\right)\boldsymbol{k}_2 - \left(\frac{s_{12}}{P}\right)\boldsymbol{k}_1. \tag{3.44}$$

The reciprocal superlattice is P times "denser" than the fundamental reciprocal lattice $\mathcal{L}^*$ [see Fig. 3(c)], i.e., the area of its unit cell is P times smaller and is equal to $(2\pi)^2/(PS_0)$. Correspondingly, the equation that is inverse to Eq. (3.42) holds for reciprocal lattices. Namely, one can choose P shift wave vectors $\boldsymbol{\kappa}_p \in \mathcal{SL}^*$, $p \in [1, P]$, such that

$$\mathcal{SL}^* = \bigcup_p \{\boldsymbol{k} + \boldsymbol{\kappa}_p \,|\, \boldsymbol{k} \in \mathcal{L}^*\}. \tag{3.45}$$

The choice of the shift vectors $\boldsymbol{\delta}_p$ and $\boldsymbol{\kappa}_p$ is not unique. Besides the freedom in the order of enumeration of the shift vectors, the real-space vectors $\boldsymbol{\delta}_p$ are defined to the accuracy of the superlattice vector $\mathcal{SL}$, whereas the wave vectors $\boldsymbol{\kappa}_p$ can be shifted by an arbitrary vector of the fundamental reciprocal lattice $\mathcal{L}^*$.

Each dot at the position j_p belongs to a certain $p \in [1, P]$ superlattice [in the sense of Eq. (3.42)]. The equilibrium directions of the magnetizations $\boldsymbol{\mu}_j$ and internal fields B_j depend only on the index p,

$$\boldsymbol{\mu}_{j_p} = \boldsymbol{\mu}_p, \quad B_{j_p} = B_p. \tag{3.46}$$

Then, the general equilibrium condition, Eq. (3.6), reduces to P vector equations,

$$B_p\boldsymbol{\mu}_p = \boldsymbol{B}_e - \mu_0 M_s \sum_q \hat{\boldsymbol{G}}_{\boldsymbol{0}}(\boldsymbol{\delta}_{pq}) \cdot \boldsymbol{\mu}_q, \tag{3.47}$$

where

$$\boldsymbol{\delta}_{pq} = \boldsymbol{\delta}_p - \boldsymbol{\delta}_q \tag{3.48}$$

and

$$\hat{\boldsymbol{G}}_{\boldsymbol{0}}(\boldsymbol{\delta}) = \sum_{\boldsymbol{r} \in \mathcal{SL}} \hat{\boldsymbol{N}}(\boldsymbol{r} + \boldsymbol{\delta}). \tag{3.49}$$

The meaning of the subscript $\boldsymbol{0}$ will be explained below.

The linear spin-wave excitations in a superlattice have the form of plane waves and can be written as

$$\boldsymbol{m}_{j_p} = \boldsymbol{m}_{\boldsymbol{k},p} e^{i\boldsymbol{k}\cdot\boldsymbol{r}_{j_p}}, \tag{3.50}$$

where the wave vector $\boldsymbol{k}$ belongs to the first Brillouin zone of the reciprocal superlattice $\mathcal{SL}^*$. Using the ansatz, Eq. (3.50),

in Eq. (3.12) one can obtain a finite-dimensional eigenvalue problem for $\omega_{\boldsymbol{k}}$ and $\boldsymbol{m}_{\boldsymbol{k},p}$:

$$-i\omega_{\boldsymbol{k}}\boldsymbol{m}_{\boldsymbol{k},p} = \boldsymbol{\mu}_p \times \sum_q \hat{\boldsymbol{\Omega}}_{\boldsymbol{k},pq} \cdot \boldsymbol{m}_{\boldsymbol{k},q}. \tag{3.51}$$

Here

$$\hat{\boldsymbol{\Omega}}_{\boldsymbol{k},pq} = \gamma B_p \delta_{pq} \hat{\boldsymbol{I}} + \gamma\mu_0 M_s \hat{\boldsymbol{G}}_{\boldsymbol{k}}(\boldsymbol{\delta}_{pq}), \tag{3.52}$$

where

$$\hat{\boldsymbol{G}}_{\boldsymbol{k}}(\boldsymbol{\delta}) = \sum_{\boldsymbol{r}\in\mathcal{SL}} \hat{\boldsymbol{N}}(\boldsymbol{r}+\boldsymbol{\delta}) e^{-i\boldsymbol{k}\cdot(\boldsymbol{r}+\boldsymbol{\delta})}. \tag{3.53}$$

As one can see, for $\boldsymbol{k} = \boldsymbol{0}$ the definition, Eq. (3.53), coincides with Eq. (3.49). Changing the summation from the direct $\mathcal{SL}$ to the reciprocal $\mathcal{SL}^*$ lattice [see Eq. (3.34)], one gets

$$\hat{\boldsymbol{G}}_{\boldsymbol{k}}(\boldsymbol{\delta}) = \frac{1}{PS_0} \sum_{\boldsymbol{K}\in\mathcal{SL}^*} \hat{\boldsymbol{N}}_{\boldsymbol{k}+\boldsymbol{K}} e^{i\boldsymbol{K}\cdot\boldsymbol{\delta}}. \tag{3.54}$$

The tensor $\hat{\boldsymbol{G}}_{\boldsymbol{k}}(\boldsymbol{\delta})$ is symmetric with respect to the transposition of the vector indices ($\hat{\boldsymbol{G}}^{\mathrm{T}}_{\boldsymbol{k}} = \hat{\boldsymbol{G}}_{\boldsymbol{k}}$) but, in general, is neither real nor symmetric in respect to inversion. Instead, one can prove the following general symmetry properties of this tensor:

$$\hat{\boldsymbol{G}}_{\boldsymbol{k}}(\boldsymbol{\delta}) = \hat{\boldsymbol{G}}^*_{-\boldsymbol{k}}(\boldsymbol{\delta}) = \hat{\boldsymbol{G}}^*_{\boldsymbol{k}}(-\boldsymbol{\delta}) = \hat{\boldsymbol{G}}_{-\boldsymbol{k}}(-\boldsymbol{\delta}). \tag{3.55}$$

In addition, $\hat{\boldsymbol{G}}_{\boldsymbol{k}+\boldsymbol{k}_S}(\boldsymbol{\delta}) = \hat{\boldsymbol{G}}_{\boldsymbol{k}}(\boldsymbol{\delta}) e^{-i\boldsymbol{k}_S\cdot\boldsymbol{\delta}}$ for any reciprocal wave vector $\boldsymbol{k}_S \in \mathcal{SL}^*$.

Using Eq. (3.45), we can rewrite in Eq. (3.55) the sum over the reciprocal superlattice $\mathcal{SL}^*$ as P sums over the fundamental reciprocal lattice $\mathcal{L}^*$:

$$\hat{\boldsymbol{G}}_{\boldsymbol{k}}(\boldsymbol{\delta}) = \frac{1}{PS_0} \sum_p \sum_{\boldsymbol{K}\in\mathcal{L}^*} \hat{\boldsymbol{N}}_{\boldsymbol{k}+\boldsymbol{\kappa}_p+\boldsymbol{K}} e^{i(\boldsymbol{\kappa}_p+\boldsymbol{K})\cdot\boldsymbol{\delta}}. \tag{3.56}$$

Note, that $\boldsymbol{\delta}_{pq} = \boldsymbol{\delta}_p - \boldsymbol{\delta}_q$ in Eq. (3.53) belongs to the fundamental lattice and, respectively,

$$e^{i\boldsymbol{K}\cdot\boldsymbol{\delta}_{pq}} = 1, \tag{3.57}$$

for any wave vector $\boldsymbol{K} \in \mathcal{L}^*$. This fact allows one to rewrite $\hat{\boldsymbol{G}}_{\boldsymbol{k}}(\boldsymbol{\delta})$ in the following final form:

$$\hat{\boldsymbol{G}}_{\boldsymbol{k}}(\boldsymbol{\delta}) = \frac{1}{P} \sum_p \hat{\boldsymbol{F}}_{\boldsymbol{k}+\boldsymbol{\kappa}_p} e^{i\boldsymbol{\kappa}_p\cdot\boldsymbol{\delta}}. \tag{3.58}$$

It is useful to note that $e^{i\boldsymbol{\kappa}_p\cdot\boldsymbol{\delta}}$ is a Pth-order root of 1, i.e., $\boldsymbol{\kappa}_p \cdot \boldsymbol{\delta} = 2\pi n/P$, where n is an integer number.

The tensor $\hat{\boldsymbol{G}}_{\boldsymbol{k}}(\boldsymbol{\delta})$ describes both static [see Eq. (3.47)] and dynamic [Eqs. (3.51) and (3.52)] properties of the magnetic dot array in a complex periodic state. Equation (3.58) represents this tensor as a *finite* sum (P terms) of the fundamental tensors $\hat{\boldsymbol{F}}_{\boldsymbol{k}}$ calculated at different points of the wave-vector space. Thus, the fundamental tensor $\hat{\boldsymbol{F}}_{\boldsymbol{k}}$ allows one to analytically describe *all* the properties of *any* periodic ground state of a magnetic dot array.

For a fixed value of the wave vector $\boldsymbol{k}$, the eigenvalue problem, Eq. (3.51), is a $2P$-dimensional linear system of equations. It has $2P$ solutions, which can be enumerated using a discrete index λ. As usual, one half of the solutions corresponds to physical modes having positive norms $A_{\boldsymbol{k},\lambda} > 0$, while the other half are formal conjugated modes with $A_{\boldsymbol{k},\lambda} < 0$, so the spin-wave spectrum contains P branches. In analyzing the properties of spin-wave modes in an infinite array [e.g., Eqs. (3.14) and (3.23)], the infinite sum over the dot index j can be replaced by the finite sum over the superlattice index p. For instance, the orthogonality condition, Eq. (3.14), will have the following form:

$$\sum_p \boldsymbol{m}^*_{\boldsymbol{k},\lambda,p} \cdot \boldsymbol{\mu}_p \times \boldsymbol{m}_{\boldsymbol{k},\lambda,p} = -iA_{\boldsymbol{k},\lambda}\delta_{\lambda,\lambda'}, \tag{3.59}$$

whereas the damping rate $\Gamma_{\boldsymbol{k},\lambda}$ is given by

$$\Gamma_{\boldsymbol{k},\lambda} = \alpha_G \omega_{\boldsymbol{k},\lambda} \left(\frac{1}{A_{\boldsymbol{k},\lambda}} \sum_p \boldsymbol{m}^*_{\boldsymbol{k},\lambda,p} \cdot \boldsymbol{m}_{\boldsymbol{k},\lambda,p} \right). \tag{3.60}$$

The absorption spectra are, also, described by Eqs. (3.27) and (3.28), where the summation over the dots is replaced by the summation over the superlattices and only the modes with zero wave vector $\boldsymbol{k} = \boldsymbol{0}$ are taken into account.

IV. EXAMPLES: APPLICATIONS OF THE GENERAL THEORY IN SEVERAL PARTICULAR CASES

In this section the above-described general formalism will be used for the calculation of the spectra of collective spin-wave modes in several particular cases. We will consider an array of circular cylindrical magnetic dots having radius R and height h [see Fig. 4(a)] arranged in a square lattice with the lattice constant a [see Fig. 4(b)]. We will focus mainly on the case of "long" cylinders ($h > 2R$), when, in the absence of the bias magnetic field, the equilibrium magnetization direction $\boldsymbol{\mu}$ is directed along the dot's axis of symmetry [see Fig. 4(a)].

A. Ferromagnetic state of the magnetic dot array

First, we consider a "perpendicular" ferromagnetic (FM) ground state of the array, in which equilibrium directions of magnetizations of all the dots are aligned along the z axis, $\boldsymbol{\mu} = \boldsymbol{e}_z$. Note, that the area of the unit cell of the square lattice is $S_0 = a^2$ and the basis wave vectors of the reciprocal lattice [see Eq. (3.37)] are given by

$$\boldsymbol{k}_1 = \frac{2\pi}{a}\boldsymbol{e}_x\,, \quad \boldsymbol{k}_2 = \frac{2\pi}{a}\boldsymbol{e}_y\,. \tag{4.1}$$

This allows us to directly calculate the fundamental tensor $\hat{\boldsymbol{F}}_{\boldsymbol{k}}$ using Eq. (3.35). The spin-wave spectrum in the FM state is described by the general equation (3.38). Note, that in the considered case ($\boldsymbol{\mu} = \boldsymbol{e}_z$) the primed coordinate system ($x'y'z'$) in Eq. (3.38) coincides with the unprimed one (xyz).

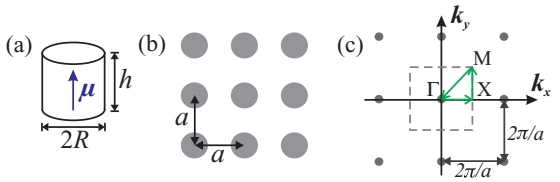

FIG. 4. (Color online) (a) Geometry of the nanodots. (b) Square lattice of the array. (c) Reciprocal lattice (gray circles) of the array. Dashed line—boundary of the first Brillouin zone in the ferromagnetic state. Green arrows show the contour $\Gamma \to X \to M \to \Gamma$ of the spectrum plot in Fig. 5.

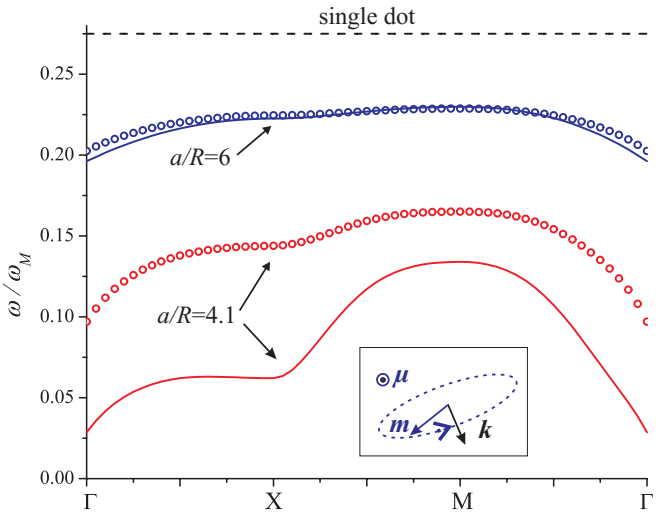

FIG. 5. (Color online) Spectra of collective spin waves of a square array of cylindrical magnetic dots (aspect ratio is $h/R = 5$) in a FM ground state without external magnetic field. The contour $\Gamma \to X \to M \to \Gamma$ is shown in Fig. 4(c). Open circles—calculations using Eq. (3.38) with account of the real shape of the nanodots; solid lines—calculations in point-dipole approximation (Ref. 24). The lower pair of curves corresponds to the array's lattice constant $a = 4.1R$ and the upper pair to $a = 6R$. The upper dashed line shows the resonance frequency of a single dot. Inset: vector structure of the dynamical magnetization $\boldsymbol{m}_{\boldsymbol{k}}$ of a spin wave with wave vector $\boldsymbol{k}$.

The calculated spectra of collective spin waves in a magnetic dot array in the perpendicular FM ground state in the absence of the external field are shown in Fig. 5 by open circles [for definition of the symmetric points Γ, X, and M of the first Brillouin zone, see Fig. 4(c)]. Solid lines in Fig. 5 show, for comparison, spin-wave spectra for an array of *point dipoles*[24] having the same magnetic moment per dot.

As one can see from Fig. 5, for relatively large separation a between the dots the spectrum is monotonic in the whole Brillouin zone. For a smaller separation, the spectrum becomes nonmonotonic—a local frequency minimum appears at $\boldsymbol{k} = \{\pi/a, 0\}$ (point X). With further reduction of the separation a the frequency in the X point becomes complex, and the FM state loses stability. This corresponds to the transition into a chessboard antiferromagnetic state. The corresponding region of stability of the FM ground state will be shown in Sec. IV C.

It can also be seen from Fig. 5 that the spin-wave spectra of the array calculated in the model of point dipoles[24] are qualitatively similar to the spectra calculated with account of real shape of the magnetic dots (compare solid lines and open circles in Fig. 5). At the same time, the two models agree quantitatively only for rather large separations a, when the dynamic dipolar coupling (proportional to the width of the spin-wave band) is weak. In particular, the point-dipole model substantially underestimates the region of stability of the FM state. Thus, although the point-dipole model can be used for a qualitative analysis of spin-wave spectra in magnetic arrays, the quantitatively correct calculations require account of the real shape of the dots.

The excitations $\boldsymbol{m}_{\boldsymbol{k}}$ of the array in the FM state are plane waves with right elliptic polarization (only in the two symmetric points Γ and M the polarization is circular). The major axis of the polarization ellipse is perpendicular to the wave vector $\boldsymbol{k}$ (see inset in Fig. 5). In accordance with Eq. (3.60), this ellipticity causes the increase in the spin-wave damping rate, but our calculations showed that these changes are rather small—the difference between $\Gamma_{\boldsymbol{k}}$ and $\alpha_G \omega_{\boldsymbol{k}}$ exceeds 10% only in a small region near the boundary of stability of the FM state.

Using Eq. (3.38) and noting that the off-diagonal components of the tensor $\hat{\boldsymbol{F}}_{\boldsymbol{k}}$ vanish at $\boldsymbol{k} = \boldsymbol{0}$, one can derive a simple expression for the ferromagnetic resonance (FMR) frequency of the square dot array in a perpendicular bias field $\boldsymbol{B}_e = B_e \boldsymbol{e}_z$:

$$\omega_{\mathrm{FMR}} = \gamma B_e + \omega_M \left(F_{\boldsymbol{0}}^{(xx)} - F_{\boldsymbol{0}}^{(zz)} \right). \tag{4.2}$$

In the long-wavelength limit $\boldsymbol{k} \to \boldsymbol{0}$ the spin-wave spectrum is isotropic and has nonanalytic peculiarity (which means that the spin waves have a finite group velocity at $\boldsymbol{k} \to \boldsymbol{0}$). The long-wavelength approximation of the dispersion relation $\omega_{\boldsymbol{k}}$ can be easily derived by noting that in Eq. (3.35) only the term $\hat{\boldsymbol{N}}_{\boldsymbol{k}}$ has a nonanalytic behavior near $\boldsymbol{k} = \boldsymbol{0}$, whereas all the other terms $\hat{\boldsymbol{N}}_{\boldsymbol{k}+\boldsymbol{K}}$ are regular in $\boldsymbol{k}$ and can be expanded in a Taylor series. The terms in $\hat{\boldsymbol{N}}_{\boldsymbol{k}+\boldsymbol{K}}$ that are linear in $\boldsymbol{k}$ vanish after summation over the reciprocal lattice, and the dispersion relation for small $\boldsymbol{k}$ can be written in a simple form:

$$\omega_{\boldsymbol{k}} \approx \omega_{\mathrm{FMR}} + \omega_M \frac{\pi h R^2}{4a^2} |\boldsymbol{k}| + O[(ka)^2]. \tag{4.3}$$

By comparing this expression with the dispersion equation for the magnetostatic waves propagating in a normally magnetized thin film[30] written in a long-wavelength limit one can conclude that the group velocity in both cases is exactly the same, provided that magnetic moments per unit area in both cases ($\pi R^2 h M_s / a^2$ for our case and $M_s h$ for the film) are equal.

B. Chessboard antiferromagnetic state of a magnetic dot array

As an example of a complex periodic ground state, we consider a chessboard antiferromegnetic (CAFM) ground state, in which the equilibrium magnetizations of the nearest neighbors are opposite [see Fig. 6(a)],

$$\boldsymbol{\mu}_j = (-1)^{j_x + j_y} \boldsymbol{e}_z. \tag{4.4}$$

The CAFM state is the true ground state for a square array of magnetic dots with perpendicular anisotropy (without applied field), i.e., it corresponds to the global energy minimum of the array.[7]

For the CAFM ground state, the basis vectors of the superlattice $\mathcal{SL}$ can be chosen as [see Fig. 6(a)]

$$\tilde{\boldsymbol{a}}_1 = \boldsymbol{a}_1 - \boldsymbol{a}_2, \quad \tilde{\boldsymbol{a}}_2 = \boldsymbol{a}_1 + \boldsymbol{a}_2. \tag{4.5}$$

In terms of Eq. (3.40), this corresponds to the choice $s_{11} = s_{21} = s_{22} = 1$, $s_{12} = -1$. The number of independent superlattices is, clearly,

$$P = s_{11} s_{22} - s_{12} s_{22} = 2. \tag{4.6}$$

The basis wave vectors of the reciprocal superlattice $\mathcal{SL}^*$ are given by [see Eq. (3.43)]

$$\tilde{\boldsymbol{k}}_1 = (\boldsymbol{k}_1 - \boldsymbol{k}_2)/2, \qquad \tilde{\boldsymbol{k}}_2 = (\boldsymbol{k}_1 + \boldsymbol{k}_2)/2. \tag{4.7}$$

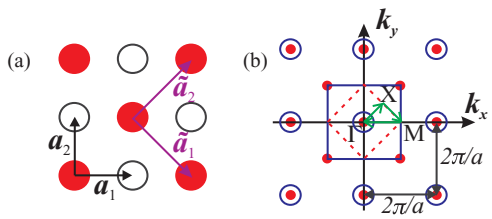

FIG. 6. (Color online) (a) Square array of magnetic dots in a CAFM ground state. Empty and filled circles represent the dots with opposite directions of the equilibrium magnetization $\boldsymbol{\mu}_j = \pm \boldsymbol{e}_z$. (b) Reciprocal lattice $\mathcal{L}^*$ (larger open circles) and reciprocal superlattice $\mathcal{SL}^*$ (smaller filled circles). The solid (dashed) lines in the middle show the boundaries of the first Brillouin zone for the reciprocal fundamental lattice (reciprocal superlattice). The solid arrows in the middle show the contour $\Gamma \to X \to M \to \Gamma$ of the spectrum plot in Fig. 7.

The reciprocal superlattice $\mathcal{SL}^*$ is shown in Fig. 6(b) in comparison with the fundamental reciprocal lattice $\mathcal{L}^*$. The area of the first Brillouin zone of the superlattice $\mathcal{SL}^*$ is $P = 2$ times smaller than the area of the first Brillouin zone of the fundamental lattice $\mathcal{L}^*$.

The shift vectors $\boldsymbol{\delta}_p$ and wave vectors $\boldsymbol{\kappa}_p$ can be chosen as

$$\boldsymbol{\delta}_1 = \mathbf{0}, \quad \boldsymbol{\delta}_2 = \boldsymbol{a}_1, \tag{4.8a}$$

$$\boldsymbol{\kappa}_1 = \mathbf{0}, \quad \boldsymbol{\kappa}_2 \equiv \boldsymbol{\kappa} = (\boldsymbol{k}_1 + \boldsymbol{k}_2)/2. \tag{4.8b}$$

One can check by direct substitution that Eqs. (3.42) and (3.45) are satisfied with this choice of $\boldsymbol{\delta}_p$ and $\boldsymbol{\kappa}_p$.

Noting that $e^{\pm i \boldsymbol{a}_1 \cdot \boldsymbol{\kappa}} = -1$, one can simplify expressions for the interaction tensors $\hat{\boldsymbol{G}}_{\boldsymbol{k}}(\boldsymbol{\delta}_{pq})$ [see Eq. (3.58)] to

$$\hat{\boldsymbol{G}}_{\boldsymbol{k}}(\mathbf{0}) = \tfrac{1}{2}(\hat{\boldsymbol{F}}_{\boldsymbol{k}} + \hat{\boldsymbol{F}}_{\boldsymbol{k}+\boldsymbol{\kappa}}), \tag{4.9a}$$

$$\hat{\boldsymbol{G}}_{\boldsymbol{k}}(\pm \boldsymbol{a}_1) = \tfrac{1}{2}(\hat{\boldsymbol{F}}_{\boldsymbol{k}} - \hat{\boldsymbol{F}}_{\boldsymbol{k}+\boldsymbol{\kappa}}). \tag{4.9b}$$

The tensors $\hat{\boldsymbol{G}}_{\boldsymbol{k}}(\mathbf{0})$ and $\hat{\boldsymbol{G}}_{\boldsymbol{k}}(\pm \boldsymbol{a}_1)$ describe, respectively, the self-interaction of the superlattices ($p = q = 1$ or $p = q = 2$) and the interaction between the different superlattices ($p = 1$, $q = 2$ or $p = 2$, $q = 1$).

Using Eqs. (3.47) and (4.9), the effective fields $B_{1,2}$ acting on superlattices can be written as

$$B_{1,2} = \pm B_e - \mu_0 M_s F_{\boldsymbol{\kappa}}^{(zz)}. \tag{4.10}$$

Here, the first $p = 1$ superlattice has the equilibrium magnetization direction in the $+z$ direction, i.e., $\boldsymbol{\mu}_1 = \boldsymbol{e}_z$ and $\boldsymbol{\mu}_2 = -\boldsymbol{e}_z$.

Then, the eigenvalue problem, Eq. (3.51), is simplified to

$$\mp i\omega_{\boldsymbol{k}} \boldsymbol{m}_p = \boldsymbol{e}_z \times \left(\gamma B_p + \frac{\omega_M}{2} [\hat{\boldsymbol{F}}_{\boldsymbol{k}} + \hat{\boldsymbol{F}}_{\boldsymbol{k}+\boldsymbol{\kappa}}] \right) \boldsymbol{m}_p + \frac{\omega_M}{2} \boldsymbol{e}_z \times [\hat{\boldsymbol{F}}_{\boldsymbol{k}} - \hat{\boldsymbol{F}}_{\boldsymbol{k}+\boldsymbol{\kappa}}] \boldsymbol{m}_q, \tag{4.11}$$

where $p,q = 1,2$, $q \neq p$. The characteristic equation of the system (4.11) is, in fact, biquadratic, having two pairs of conjugated solutions (two physical branches and two conjugated ones). In the most important case $\boldsymbol{k} = \mathbf{0}$ (only such modes can be excited by a spatially uniform microwave field) both tensors $\hat{\boldsymbol{F}}_{\boldsymbol{k}}$ and $\hat{\boldsymbol{F}}_{\boldsymbol{k}+\boldsymbol{\kappa}}$ become diagonal, which allows one to derive a simple explicit expression for the FMR frequencies

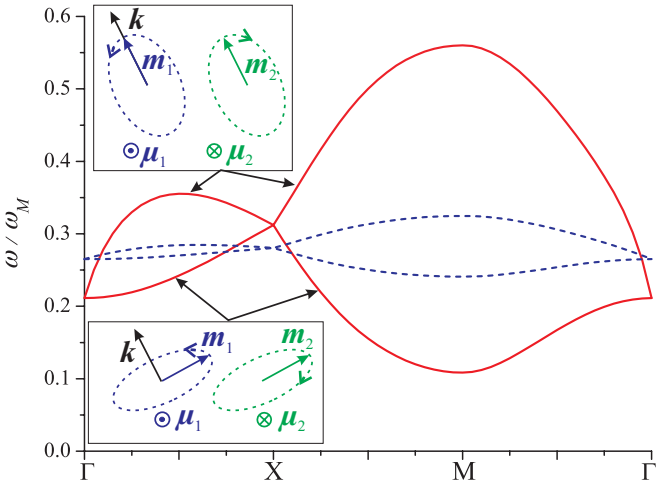

FIG. 7. (Color online) Spectra of collective spin waves of a square array of cylindrical magnetic dots (aspect ratio is $h/R = 5$) in a CAFM ground state without external magnetic field. The solid (red) lines correspond to the lattice constant $a = 2.5R$, while the blue dashed lines correspond to $a = 5R$. Insets: vector structures of dynamical magnetization $\boldsymbol{m}_p$ of the high-frequency (upper inset) and low-frequency (lower inset) spin-wave branches.

of the square array in the CAFM ground state:

$$\omega_{\mathrm{FMR}} = \omega_M \sqrt{\left(F_{\boldsymbol{\kappa}}^{(xx)} - F_{\boldsymbol{\kappa}}^{(zz)}\right)\left(F_{\mathbf{0}}^{(xx)} - F_{\boldsymbol{\kappa}}^{(zz)}\right)} \pm \gamma B_e. \tag{4.12}$$

It should be noted that another possible antiferromagnetic state—a stripe antiferromagnetic state (SAFM), $\boldsymbol{\mu}_j = (-1)^{j_x} \boldsymbol{e}_z$—can be analyzed in an absolutely analogous way [in particular, the FMR frequencies are given by the same Eq. (4.12)]. The only substantial difference with the case of a CAFM ground state is that for the SAFM state $\boldsymbol{\kappa} = \boldsymbol{k}_1/2$.

The two (low-frequency and high-frequency) spin-wave branches of the CAFM state calculated in the absence of the bias magnetic field ($B_e = 0$) are shown in Fig. 7. The branches are degenerate at two points of the Brillouin zone (Γ and X points). The degeneracy at Γ point ($\boldsymbol{k} = \mathbf{0}$) is connected with 90° rotational symmetry of the square lattice and will be absent, for example, in an array having rectangular lattice or elliptical shape of the dots. The degeneracy at the X point ($\boldsymbol{k} = \boldsymbol{\kappa}/2 = \{\pi/(2a), \pi/(2a)\}$) is of a more general nature. Using the general symmetry properties of the tensor $\hat{\boldsymbol{F}}_{\boldsymbol{k}}$ one can prove that $\hat{\boldsymbol{F}}_{\boldsymbol{\kappa}/2+\boldsymbol{\kappa}} = \hat{\boldsymbol{F}}_{-\boldsymbol{\kappa}/2} = \hat{\boldsymbol{F}}_{\boldsymbol{\kappa}/2}$. Then, the system of equations (4.11) splits into two identical independent equations. In other words, at this point the two sublattices do not interact with each other. Thus, the degeneracy at $\boldsymbol{k} = \boldsymbol{\kappa}/2$ will be present in arrays having an arbitrary oblique lattice in zero bias magnetic field. The application of a perpendicular bias field B_e, of course, removes the degeneracy of the spin-wave branches, as evident from Eq. (4.12).

The lower spin-wave branch has a local minimum in the M point (see Fig. 7). With decreasing aspect ratio h/R of the dots or decreasing lattice constant a the spin-wave frequency at this point monotonically decreases. When it reaches zero, the CAFM state loses its stability, and the array switches to a

collinear antiferromagnetic in-plane state (for details and exact definitions, see Ref. 8).

The vector structure of the spin-wave modes in the CAFM ground state is shown in the insets in Fig. 7. The magnetic moments of the neighboring dots (having opposite directions of the static magnetization) rotate in opposite directions following the similar elliptic trajectories. For the low-frequency branch, the major axis of the precession ellipse is perpendicular to the wave vector $\boldsymbol{k}$, whereas for the high-frequency branch it changes from the parallel to $\boldsymbol{k}$ near the center of the Brillouin zone to the perpendicular one near its edges (see inset in Fig. 7). The sum of eigenvectors $\boldsymbol{m}_1$ and $\boldsymbol{m}_2$ forms a linearly polarized wave with polarization parallel (perpendicular) to $\boldsymbol{k}$ for the high-frequency (low-frequency) spin-wave branch.

Similar to the situation in the FM ground state, the spin-wave damping in the CAFM state is close to $\alpha_G\omega_k$ except for a rather small region near the boundary of stability of the CAFM state. Note, that, in general, due to the existence of off-diagonal terms in Eq. (3.22) damping can cause splitting of frequencies of the spin-wave modes at the degenerate points. However, in the above-considered case the degenerate spin waves are orthogonal to each other, and the off-diagonal damping terms vanish, $\Gamma_{\nu,\nu'} = 0$ for $\nu \neq \nu'$.

C. Multistability and possibility of dynamic control of the array's ground states

It was discussed above that FM and CAFM ground states of the magnetic dot array remain stable within certain intervals of variation of the dot aspect ratio h/R and the dimensionless array lattice constant a/R and lose their stability outside of these intervals. The stability diagram of ground states calculated for an array of identical cylindrical dots coupled by magnetodipole interaction is shown in Fig. 8. Obviously, for infinitely large interdot separation a both FM and CAFM ground states are stable if the dot aspect ratio exceeds a critical value $h/R > \beta_{cr} \approx 1.81$, at which the ground states of a single dot with an in-plane and out-of-plane magnetization have the same energy.[31] If the dot aspect ratio is smaller than this critical value, the static magnetization of an individual dot will be lying in the dot plane, and an "in-plane" ground state of a dot array will be realized. When the interdot distance a/R is decreasing the critical aspect ratio h/R increases for both FM and CAFM ground states, but with a different slope, and, in the case of a very dense array, where dots are practically touching each other ($a/R \to 2$), only the CAFM ground state remains stable.

At the same time, there is a large interval of the dot's and array's parameters where both FM and CAFM ground states of the array are stable *simultaneously*. The properties of spin-wave excitations in these two ground states of the array are substantially different. In particular, these states have different frequencies of the FMR, which may be important for the practical applications of magnetic dot arrays.

Our estimations have shown that in a dot array having parameters that are not too close to the boundaries of the ground state stability the difference between the FMR frequencies in the FM and CAFM ground states can substantially exceed the FMR linewidth in the dot material and, therefore, the different microwave absorption lines in the FM and CAFM states could be observed experimentally. In particular, for an array of permalloy dots with the aspect ratio $h/R = 5$, interdot separation $a/R = 4$, static magnetization $\mu_0 M_s = 1.07$ T ($\omega_M/2\pi \approx 30$ GHz), and Gilbert damping parameter $\alpha_G = 0.01$ the difference between the FMR frequencies in the FM and CAFM ground states can be of the order of $0.1\omega_M$ (about 3 GHz) when the FMR frequencies themselves are of the order of $(0.2\text{–}0.3)\,\omega_M$ and the FMR linewidth does not exceed 50 MHz (see inset of Fig. 8). It is clear from Fig. 8 that the microwave absorbtion spectra in the FM and CAFM states of the array of Py dots have well-defined, distinct peaks that are easy to detect in a standard microwave experiment.

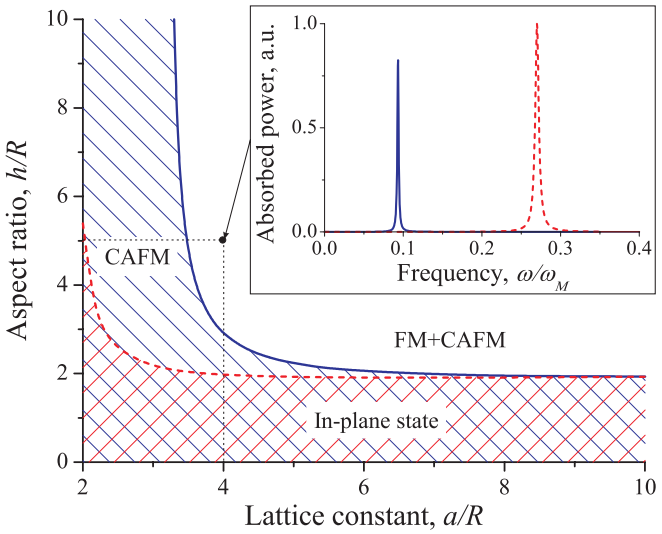

FIG. 8. (Color online) Regions of stability of different ground states of a magnetic dot array in zero applied field: above the solid blue line both the FM and the CAFM ground states are stable; below the solid blue line, but above the dashed red line only the CAFM ground state is stable; below the dashed red line both FM and CAFM states are unstable and array switches to a state with in-plane direction of the dot static magnetization. Black dot indicates the point at which the absorption spectra shown in the inset were calculated. Inset: normalized spin-wave absorption spectra of the array of permalloy cylindrical dots in the FM (solid blue curve) and CAFM (dashed red curve) ground states. Parameters: $a/R = 4$, $h/R = 5$, $\omega_M/2\pi \approx 30$ GHz, $\alpha_G = 0.01$, polarization of the exciting microwave field—linear in the array's plane.

It is important to note that in the parameter region where both ground states of an array are stable it is possible to switch the array between the ground states by applying an external bias magnetic field. The switching to the ferromagnetic ground state is trivial—one needs to apply a sufficiently large bias field that is perpendicular to the dot plane. The switching to the antiferromagnetic ground state is more complicated, but the fact that the CAFM state corresponds to the global energy minimum of the array, helps to understand how this switching can be performed. If, for example, we would bring the dot array existing in the FM state to an unstable state with maximum energy (where all the dot magnetizations are oriented in-plane) by applying a sufficiently large in-plane bias magnetic field and then removing it, the most probable final ground state of the array will be chessboard antiferromagnetic.

The determination of the exact parameters (such as amplitude and duration) of the in-plane magnetic field pulse that would guarantee switching from the FM to the CAFM ground state represents an independent nontrivial problem that is beyond the scope of the current work.

D. Localized spin-wave modes caused by a local defect in a periodic array of magnetic dots

The above-discussed ideal periodic ground states of a magnetic dot array cannot be realized in practice, since, first of all, any real experimental array is finite in size. Also, many types of local defects, such as a domain wall, presence in the array of a dot having a different size, or an absence of the dot at one of the regular dot locations can exist in the array. However, if the density of local defects is sufficiently small, the global properties of the array may stay almost the same as in the perfect periodic case. In such a case of relatively "rare" defects one may expect only a weak change in the main spin-wave spectra of the array compared to the spectra of a "rigorously periodic" array, but also, the appearance in this spectrum of novel localized spin-wave modes associated with the existence of a particular defect.

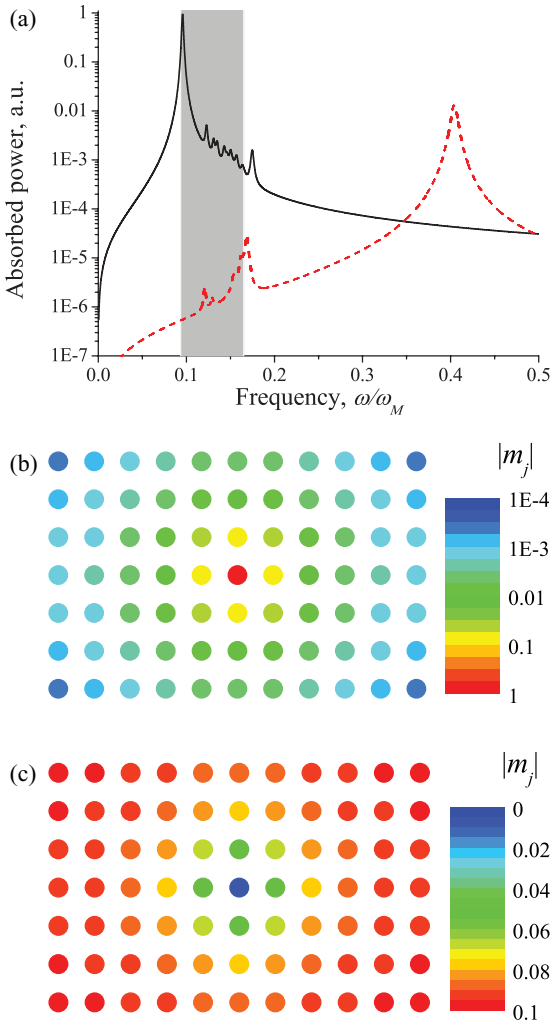

FIG. 9. (Color online) Spin-wave absorption spectra (a) and mode structure [(b) and (c)] in a magnetic dot array in a FM ground state having one defect per 11 × 11 dots. Dot aspect ratio $h/R = 5$; lattice constant $a/R = 4$. (a) Solid curve—absorption spectrum for the microwave signal having right in-plane polarization [i.e., $\boldsymbol{b}_e = (b\cos\omega t, b\sin\omega t, 0)$]. The main peak at $\omega = 0.095\omega_M$ corresponds to the FMR frequency of the array. Dashed curve—absorption spectrum for the signal having left in-plane polarization. The peak at $\omega = 0.4\omega_M$ corresponds to the localized defect spin-wave mode. Gray area—region of existence of spin-wave modes in a perfect (without defect) dot array. (b),(c) Spatial profiles of the localized ($\omega = 0.4\omega_M$) and FMR ($\omega = 0.095\omega_M$) spin-wave modes in the dot array with a defect.

To illustrate this idea and, also, to demonstrate the power of the above-developed general analytic approach we will consider below one particular type of a local defect, namely, when one of the dots in the array existing in the FM ground state has the magnetization direction that is opposite to the magnetization direction of all the other dots in the array. In other words, the eigenvalue problem, Eq. (3.51), will be solved with all the dot magnetizations except one directed as $\boldsymbol{\mu}_j = \boldsymbol{e}_z$, and the remaining "defective" dot has static magnetization $\boldsymbol{\mu}_{j_d} = -\boldsymbol{e}_z$. To avoid the influence of the edge effects, we will use the periodic boundary condition in the array (so, formally, a periodic ground state with a periodic local defect will be considered). For a sufficiently large distance between the defects ($\geqslant 10\,a$ for typical dot parameters) the interaction between them is negligible and this approach accurately imitates a single isolated defect in an infinite array.

The spin-wave absorption spectra and the mode structure in a dot array in the FM ground state with an isolated defect are shown in Fig. 9. As one can see from Fig. 9, the presence of an isolated defect (dot with opposite magnetization direction) in the FM dot array only weakly changes the spectrum of the fundamental spin-wave modes in the array: the mode's frequencies simply increase slightly. These changes are mainly caused by the static demagnetization field of the defect. Also, the defect creates a certain spatial nonuniformity in the profiles of the fundamental modes [an example of such a profile for the mode with $\boldsymbol{k} = \boldsymbol{0}$ is shown in Fig. 9(c)]. Due to this defect-related spatial nonuniformity the uniform spin waves with nonzero wave vectors could be excited by a uniform microwave field with right polarization (the natural polarization for the state without defects).

Obviously, the magnetization of a defect dot precesses in the direction which is opposite to the precession direction of all the other dots. Thus, the eigenmode associated with the defect can be effectively excited by the left-polarized microwave field. This defect mode is strongly localized near the defect, and the amplitude of this mode (mostly related to the amplitude of precession of magnetization $|\boldsymbol{m}_j|$ in the defect dot) decreases exponentially with the distance from the defect [see Fig. 9(b)]. Because of the larger value of the internal field near the defect the frequency of the defect mode lies higher than the main (fundamental) spectrum. The ratio of the intensities of the defect mode (excited by the left-polarized microwave field) and the fundamental mode (excited the by right-polarized microwave field) is approximately equal to the relative density of defects in the dot array. Also, the spatially uniform left-polarized microwave field excites modes with $\boldsymbol{k} \neq \boldsymbol{0}$ with rather low amplitudes, because the overlap integral between the field and the profiles of these modes is small

and the polarization of the modes is elliptical. Obviously, the fundamental mode with $\boldsymbol{k} = \boldsymbol{0}$ and right circular polarization cannot be excited by such a microwave field.

Thus, if the external microwave signal is spatially uniform and has right circular polarization the absorption properties of the dot array in respect to this signal are not substantially influenced by the presence of a localized defect. At the same time, measurements of the absorption spectrum for the left-polarized microwave magnetic field can be used as an effective characterization tool to find the density and types of different defects in a dot array.

V. CONCLUSIONS

The general formalism developed in our current paper allows one to investigate theoretically linear magnetization dynamics in an arbitrary array of magnetic dots coupled by magnetodipolar interaction. In the calculations presented above we restricted ourselves to the case of identical magnetic dots and used a macrospin approximation for the magnetization of individual dots. Thus, our calculations cover only the collective spin-wave modes of the array formed by spatially uniform modes of the individual dots when these dots have spatially uniform static magnetization (ground state). Both these restrictions can be relaxed by using the exact spatially nonuniform profile of spin-wave modes of individual dots in calculations of the demagnetization tensor and by introducing more than one effective demagnetization tensor $\hat{\boldsymbol{N}}$.

Since the calculations of the spin-wave spectra in finite and infinite periodic arrays of magnetic dots are formally identical, the properties of resulting collective spin-wave modes of the array are similar. In the latter case of a spatially periodic array of magnetic dots we find the collective excitations of the dot sublattices, and the role of the mutual demagnetization tensor $\hat{\boldsymbol{N}}(\boldsymbol{r})$ is played by the tensor $\hat{\boldsymbol{F}}_{\boldsymbol{k}}$. These tensors contain all the necessary information about the array's geometry. In a general case the spectrum and the profiles of the spin-wave modes of the array can be found from a standard eigenvalue problem.

A perturbation theory for the spin waves in the dot array was also developed, and this theory allows one to investigate such practically important phenomena as damping of spin-wave modes and excitation of these modes by an external microwave field. It was shown, that, in general case, the influence of both dissipation and the external microwave field leads to the interaction between different spin-wave modes of the array. In particular, these perturbations could lead to the hybridization and frequency splitting of frequency-degenerate modes. The application of the perturbation theory also demonstrated that the dissipation parameter of a particular mode is, usually, proportional to the mode ellipticity, and is not exactly equal to the Gilbert parameter $\alpha_G\omega$.

It has also been demonstrated that the spin-wave spectra in the dot arrays existing in different initial ground states (e.g., FM and CAFM) can be substantially different. In particular, such practically important characteristics of the array as the FMR frequency and group velocity of spin waves having small wave vectors $k \ll \pi/a$ are significantly different for FM and CAFM ground states of the array. In a wide range of the array's geometric parameters the difference in FMR frequencies significantly exceeds the FMR linewidth in the magnetic material of the dot. This important property of the magnetic dot arrays opens the way for development of dynamically reconfigurable magnonic crystals based on magnetic dot arrays, where the ground state, and, therefore, the microwave properties could be rapidly switched by application of a pulse of an external bias magnetic field. It has also been demonstrated that global microwave properties of magnetic dot arrays are rather robust and the presence of isolated defects in the array cannot significantly change the characteristics of fundamental spin-wave modes of the array.

ACKNOWLEDGMENTS

This work was supported in part by Grant No. DMR-1015175 from the National Science Foundation of the USA, by the contract from the US Army TARDEC, RDECOM, by the DARPA grant "Coherent Information Transduction between Photons, Magnons, and Electric Charge Carriers," by Grant No. M/90-2010 from the Ministry of Education and Science, Youth and Sport of Ukraine, and by Grant No. F34/452-2011 from the State Fund for Fundamental Research of Ukraine.

*verrv@ukr.net

[1] *Advanced Magnetic Nanostructures*, edited by D. J. Sellmyer and R. Skomski (Springer, New York, 2006).

[2] G. Gubbiotti, M. Madami, S. Tacchi, G. Carlotti, and T. Okuno, J. Appl. Phys. **99**, 08C701 (2006).

[3] A. V. Chumak, A. A. Serga, B. Hillebrands, and M. P. Kostylev, Appl. Phys. Lett. **93**, 022508 (2008).

[4] A. V. Chumak, A. A. Serga, S. Wollf, B. Hillebrands, and M. P. Kostylev, Appl. Phys. Lett. **94**, 172511 (2009).

[5] S. Tacchi, M. Madami, G. Gubbiotti, G. Carlotti, H. Tanigawa, T. Ono, and M. P. Kostylev, Phys. Rev. B **82**, 024401 (2010).

[6] S. Tacchi, F. Montoncello, M. Madami, G. Gubbiotti, G. Carlotti, L. Giovannini, R. Zivieri, F. Nizzoli, S. Jain, A. O. Adeyeye, and N. Singh, Phys. Rev. Lett. **107**, 127204 (2011).

[7] J. E. L. Bishop, A. Yu. Galkin, and B. A. Ivanov, Phys. Rev. B **65**, 174403 (2002).

[8] K. Yu. Guslienko, Appl. Phys. Lett. **75**, 394 (1999).

[9] A. Yu. Galkin and B. A. Ivanov, JETP Lett. **83**, 383 (2006).

[10] Y. Takagaki, C. Herrmann, and E. Wiebicke, J. Phys.: Condens. Matter **20**, 225007 (2008).

[11] J. Topp, D. Heitmann, and D. Grundler, Phys. Rev. B **80**, 174421 (2009).

[12] S. Tacchi, M. Madami, G. Gubbiotti, G. Carlotti, S. Goolaup, A. O. Adeyeye, N. Singh, and M. P. Kostylev, Phys. Rev. B **82**, 184408 (2010).

[13] M. Francardi, M. Sepioni, A. Gerardino, F. Sansone, G. Gubbiotti, M. Madami, S. Tacchi, and G. Carlotti, Microelectron. Eng. **87**, 1614 (2010).

[14]R. Zivieri, F. Montoncello, L. Giovannini, F. Nizzoli, S. Tacchi, M. Madami, G. Gubbiotti, G. Carlotti, and A. O. Adeyeye, Phys. Rev. B **83**, 054431 (2011).
[15]L. Giovannini, F. Montoncello, and F. Nizzoli, Phys. Rev. B **75**, 024416 (2007).
[16]G. Gubbiotti, S. Tacchi, M. Madami, G. Carlotti, A. O. Adeyeye, and M. Kostylev, J. Phys. D: Appl. Phys. **43**, 264003 (2010).
[17]R. Arias and D. L. Mills, Phys. Rev. B **70**, 104425 (2004).
[18]P. Chu, D. L. Mills, and R. Arias, Phys. Rev. B **73**, 094405 (2006).
[19]E. Tartakovskaya, W. Kreuzpaintner, and A. Schreyer, J. Appl. Phys. **103**, 023913 (2008).
[20]M. Dvornik, P. V. Bondarenko, B. A. Ivanov, and V. V. Kruglyak, J. Appl. Phys. **109**, 07B912 (2011).
[21]A. Yu. Galkin, B. A. Ivanov, and C. E. Zaspel, Phys. Rev. B **74**, 144419 (2006).
[22]J. Shibata and Y. Otani, Phys. Rev. B **70**, 012404 (2004).
[23]A. Yu. Galkin, B. A. Ivanov, and C. E. Zaspel, J. Magn. Magn. Mater. **286**, 351 (2005).
[24]P. V. Bondarenko, A. Yu. Galkin, B. A. Ivanov, and C. E. Zaspel, Phys. Rev. B **81**, 224415 (2010).
[25]P. Politi and M. G. Pini, Phys. Rev. B **66**, 214414 (2002).
[26]M. Beleggia and M. De Graef, J. Magn. Magn. Mater. **278**, 270 (2004).
[27]O. Dmytriiev, T. Meitzler, E. Bankowski, A. Slavin, and V. Tiberkevich, J. Phys.: Condens. Matter **22**, 136001 (2010).
[28]K. Y. Guslienko, A. N. Slavin, V. Tiberkevich, and S.-K. Kim, Phys. Rev. Lett. **101**, 247203 (2008).
[29]N. W. Ashkroft and N. D. Mermin, *Solid State Physics* (Holt, Rinehart, and Winston, New York, 1976).
[30]B. A. Kalinikos and A. N. Slavin, J. Phys. C **19**, 7013 (1986).
[31]K. L. Metlov and K. Yu. Guslienko, Phys. Rev. B **70**, 052406 (2004).